Electrical Response of a Medium Containing Dissociable Impurities

ARTICLE *in* THE JOURNAL OF PHYSICAL CHEMISTRY B · MARCH 2011

Impact Factor: 3.3 · DOI: 10.1021/jp1094257 · Source: PubMed

2 AUTHORS:

Giovanni Barbero
Politecnico di Torino
307 PUBLICATIONS **3,068** CITATIONS
SEE PROFILE

Ioannis Lelidis
Université de Picardie Jules Verne
75 PUBLICATIONS **635** CITATIONS
SEE PROFILE

THE JOURNAL OF PHYSICAL CHEMISTRY B

ARTICLE

pubs.acs.org/JPCB

Electrical Response of a Medium Containing Dissociable Impurities

G. Barbero[†,‡] and I. Lelidis[§]

[†]Dipartimento di Fisica, Politecnico di Torino, Corso Duca degli Abruzzi 24, 10129 Torino, Italia

[‡]Université de Picardie Jules Verne, Laboratoire de Physique des Systèmes Complexes, 33 rue Saint-Leu 80039, Amiens, France

[§]Solid State Section, Department of Physics, University of Athens, Panepistimiopolis, Zografos, Athens 157 84, Greece

ABSTRACT: The effect of the generation−recombination phenomenon on the electrical impedance of an electrolytic cell is investigated. We show that this phenomenon could be responsible for the appearance of a plateau in the real part of the impedance of the cell. The possibility to observe the plateau, arising from the generation−recombination phenomenon, is discussed in relation to the values of the association−dissociation coefficients. The analysis is done by assuming that the generation−recombination phenomenon can be described as a chemical reaction of first order, that the sample is in the shape of a slab, and that the electrodes of the cell are perfectly blocking. To simplify the analysis, the case where only one type of ions can move is considered. The extension of the results to the more general case, in which both types of ions are mobile, is also discussed.

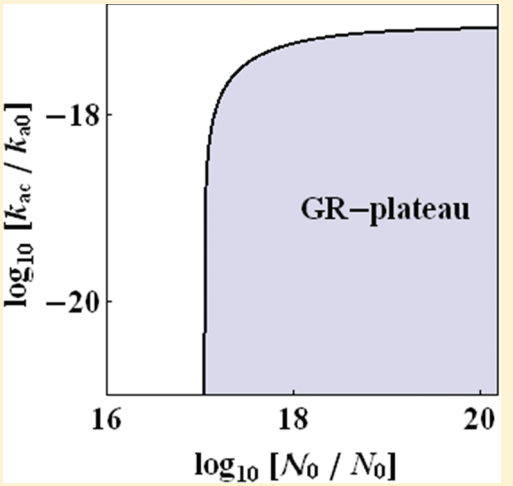

I. INTRODUCTION

The electrical properties of an electrolytic cell have been discussed long ago by Ross Macdonald in the framework of the Poisson−Nernst−Planck (PNP) model, by assuming that the electrodes of the cell are perfectly blocking.[1] The analysis presented in ref 1 is valid for the general situation where both types of ions are mobile, the ions have different charge, and the generation−recombination effect is present. In a series of articles, Ross Macdonald has investigated several aspects of the problem related to the theoretical determination of the electrical impedance of a liquid containing ions.[2] In refs 3 and 4, he discusses the effect of the absorption of ions on the electrodes on the electrical response of a sample to an external excitation. The importance of the blocking character of the electrodes on the impedance of the cell has been considered in refs 5−7. The generation−recombination effect, for its importance in the theory of semiconductors, has been also analyzed by Ross Macdonald.[8,9] In all of the articles published by Ross Macdonald, the electrical quantity evaluated is the admittance, Y, defined at the inverse of the electrical impedance, Z, of the cell. The reason is that, in the case of blocking electrodes, in the dc limit the real part, G, of Y tends to zero. The reason for using a scheme based on the admittance is also related to the natural separation of the current in a medium in displacement current and conducting current, which is useful for the separation of the dielectric constant in the real and imaginary parts.

In this framework, the phenomenon of generation−recombination of the ions is not related to peculiar electrical properties of the sample under investigation. Recently, the same problem has been reconsidered by investigating the effect of the generation−recombination phenomenon on the real and imaginary part of the impedance of the cell.[10] In that article, as in refs 8 and 11, it has been shown that the presence of the generation−recombination effect can be responsible for the appearance of a second plateau (GR plateau) in the real part of the impedance, in the case where only one type of ions is mobile. The goal of the present article is to investigate when the plateau related to the generation−recombination phenomenon is observable.

Our article is organized as follows. In section II, the main points of the PNP model are briefly discussed, and the frequency dependence of the real and imaginary parts of the impedance of a cell of liquid containing ions is discussed, in the absence of the generation−recombination phenomenon. In section III, the effect of the generation−recombination phenomenon on the electrical impedance of the cell is considered. To simplify the analysis, we limit our investigation to the case where the electrodes are blocking and only one type of ions is mobile. The spectra of the real and imaginary parts of the impedance of the cell are analyzed in section IV. Section V is devoted to the generalization of the obtained results and to the conclusions.

Received: October 1, 2010
Revised: January 26, 2011
Published: March 16, 2011

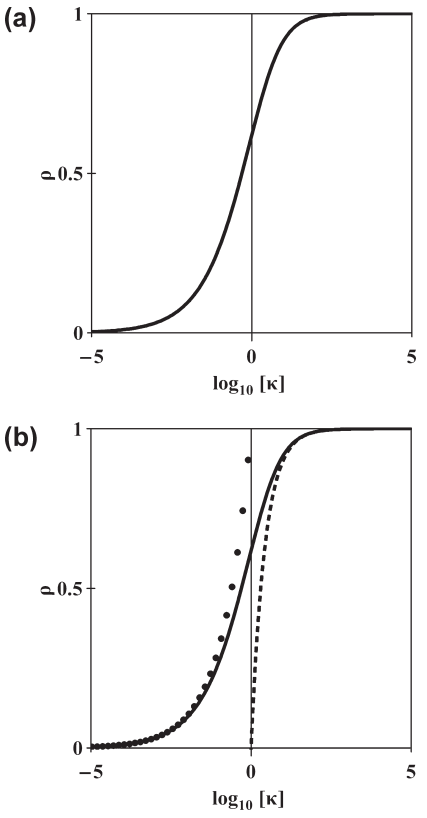

Figure 1. Dissociation ratio ρ versus $\kappa = k_d/(k_a \mathcal{N}_0)$ solid curve (a), and comparison with the approximated expressions $\rho_1 = (\kappa)^{1/2}$ and $\rho_2 = 1 - (1/\kappa)$ valid for small (solid points) and large (dashed line) κ, respectively (b).

II. FULL DISSOCIATED CASE

The PNP model is based on the differential equations representing the conservations of the positive and negative ions (continuity equations) and the relation between the electric field and the electrical charges (equation of Poisson). The boundary conditions on the electrical potential simply state that the actual potential on the electrodes has to coincide with that due to the external power supply. On the contrary, the boundary conditions on the current densities depend on the nature of the electrodes. In the case where the electrodes are perfectly blocking, as considered in our article, the current densities have to vanish on the electrodes. Other boundary conditions, related to the adsorbing character of the electrodes,[3,12] or to their ohmic character,[13,14] will not be discussed, although they could be interesting for applications. We assume that there are only two groups of ions, one positive and one negative. The anions are supposed to be immobile. This situation corresponds to a Hydro-gel where the anions are stuck on the polymeric chains, whereas the cations can move in the water. We indicate by q the modulus of the electrical charge of the ions, by ε the dielectric constant of the medium in which are dispersed the ions, by D the diffusion coefficient of the ions in the considered medium, and by $\mathcal{N}_0$ the actual bulk density of ions, in thermodynamical equilibrium. In the present section, we consider that all of the dissociable impurities are completely dissociated. Finally, we assume that the liquid is not dispersive, in the sense that, in the considered frequency region, ε can be considered frequency independent. The actual dispersion is due to the influence of the ions on the response of the cell to the external stimulus.

The applied voltage is supposed to be harmonic, $V(t) = V_0 \exp(i\omega t)$, with a small amplitude, V_0, in such a manner that the fundamental equations of the problem can be linearized, and the concept of electrical impedance valid in all frequency range $f = \omega/(2\pi)$.[15] In this situation, following the line indicated in refs 16−18, it is possible to obtain for the electrical impedance of a cell in the shape of a slab of thickness d and surface S the expression

$$Z = -i\frac{2}{\omega\varepsilon\beta^2 S}\left\{\frac{1}{\bar{\lambda}_0\beta}\tanh\left(\frac{\beta d}{2}\right) + i\frac{\omega d}{2D}\right\} \quad (1)$$

where $\bar{\lambda}_0 = (2)^{1/2}\lambda_0$, and λ_0 is the length of Debye defined by $\lambda_0 = (\varepsilon k_B T/(2\mathcal{N}_0 q^2))^{1/2}$. eq 1 was reported for the first time in ref 18 and reobtained, independently, in ref 17. Finally, the complex wave vector β is given by

$$\beta = \frac{1}{\bar{\lambda}_0}\sqrt{1 + i\omega\frac{\bar{\lambda}_0^{\,2}}{D}} \quad (2)$$

From eq 1 it follows that the effective resistance $R = \mathrm{Re}[Z]$ and reactance, $X = \mathrm{Im}[Z]$, in the series representation,

1. In the dc limit, $\omega \to 0$, tend to

$$R = \frac{\bar{\lambda}_0^{\,2} d}{\varepsilon D S}\left(1 - \frac{\bar{\lambda}_0^{\,4}}{D^2}\omega^2\right) \quad (3)$$

$$X = -2\frac{\bar{\lambda}_0}{\omega\varepsilon S}\left(1 + \frac{\bar{\lambda}_0^{\,3} d}{2D^2}\omega^2\right) \quad (4)$$

2. In the opposite limit where $\omega \to \infty$, tend to

$$R = \frac{Dd}{\omega^2\bar{\lambda}_0^2\varepsilon S}\left(1 - \frac{1}{d}\sqrt{\frac{2D}{\omega}}\right) \quad (5)$$

$$X = -\frac{d}{\omega\varepsilon S}\left(1 - \frac{D}{\bar{\lambda}_0^2 d\omega}\sqrt{\frac{2D}{\omega}}\right) \quad (6)$$

As discussed in ref 17, $R = R(\omega)$ presents a plateau ending at the circular frequency $\omega_{D0} = D/\bar{\lambda}_0^2$. For $\omega = \omega_{D0}$, $X = X(\omega)$ presents a minimum. In the low-frequency range, the electrical impedance is dominated by the ions, whereas in the high-frequency range the ions do not play any role because they do not follow the rapid time variation of the applied potential. It follows that in the high-frequency range, the medium containing the ions behaves as an insulating material. We note that the frequency separating the low-frequency from the high-frequency region is ω_{D0}, known as circular frequency of Debye. For $\omega = \omega_{D0}$, the amplitudes of the real and imaginary components of the squared complex wave vector β are equal. Clearly, the ions contribute to the real part of the conductivity σ'_∞ high-frequency plateau even though they are just oscillating over a narrow region at these frequencies.[19] So, the material is not a full insulator (pure dielectric) at these frequencies. The ions indeed play a role in the electrical response of the medium in the PNP model, even at high frequencies.[19]

dx.doi.org/10.1021/jp1094257 |J. Phys. Chem. B 2011, 115, 3496–3504

III. GENERATION−RECOMBINATION PHENOMENON

In the previous section, we have briefly discussed the influence of the ions on the electrical impedance of a cell in the shape of a slab. In that section, the bulk density of ions was fixed. This corresponds to the situation where the ions are generated by an impurity present in the gel, that is completely dissociated. This assumption holds when the bulk density of the impurity is very small with respect to the bulk density of the host medium, in such a manner that the probability of an ion to have a collision with an ion of the opposite sign is negligible. If this hypothesis is not verified, in the PNP model it is necessary to take into account also the formation and the neutralization of ions. Following the pioneering work of Ross Macdonald, we assume that the ions are formed by a neutral impurity A according to the reaction: $A = B^+ + C^-$, where B^+ and C^- are the positive and negative ions resulting from the decomposition of the neutral impurity A. By indicating with n_n, n_p, and n_m the bulk density of neutral particles, cations and anions respectively, the generation and recombination term, according to elementary kinetic theory, is represented by the terms

$$\pm (k_d n_n - k_a n_p n_m) \tag{7}$$

where the sign + holds for the generation of ions, and the sign − for the recombination. The quantities k_d and k_a are the dissociation and association coefficients, respectively. In an infinite sample, in the absence of external electric field, in thermodynamical equilibrium, the bulk density of neutral particles as well as the bulk density of ions are time and position independent. By indicating with $\mathcal{N}_0$, $\mathcal{N}_n$, and $\mathcal{N}$ the bulk densities of dissociable particles, of neutral, and of charged particles in the thermodynamical equilibrium state we have

$$\mathcal{N} + \mathcal{N}_n = \mathcal{N}_0 \text{ and } k_d \mathcal{N}_n = k_a \mathcal{N}^2 \tag{8}$$

From eq 8, it follows that the bulk density of ions, in thermodynamical equilibrium is given by

$$\mathcal{N} = \rho \mathcal{N}_0 \tag{9}$$

The dissociation ratio ρ is

$$\rho = -(\kappa/2) + \sqrt{(\kappa/2)^2 + \kappa} \tag{10}$$

where $\kappa = k_d/(k_a \mathcal{N}_0)$ is a dimensionless parameter taking into account the dissociation and association coefficient and the bulk density of dissociable particles. From eq 10, it follows that for $\kappa \to 0$, $\rho \to 0$, and for $\kappa \to \infty$, $\rho \to 1$, that is the dissociation is complete. In part a of Figure 1, we show $\rho = \rho(\kappa)$. From eq 10, we obtain that, for $\kappa \to 0$, $\rho \to \rho_1 = (\kappa)^{1/2}$, whereas for $\kappa \to \infty$, $\rho \to \rho_2 = 1 - ({}^1/_\kappa)$. In part b of Figure 1, we compare the function $\rho = \rho(\kappa)$ with the two limiting expressions reported above.

Electrical Impedance. For the present case, with only one type of mobile ions and immobile neutral impurities, solving the fundamental equations of the PNP model including the generation−recombination phenomenon, as discussed in refs 9−11 we get for the electrical impedance of the cell, in the shape of a slab of thickness d and surface area S, with perfectly blocking electrodes, the expression

$$Z = -2\frac{1}{\omega \varepsilon S \xi^2} \Upsilon \left\{ \frac{1}{\xi \bar{\lambda}^2} \tanh\left(\frac{\xi d}{2}\right) + i\frac{\omega d}{2D} \right\} \tag{11}$$

where

$$\Upsilon = \frac{i\omega + k_d + 2k_a \mathcal{N}}{i\omega + k_d + k_a \mathcal{N}} \tag{12}$$

$$\xi^2 = \frac{\Upsilon}{\bar{\lambda}^2}\left(1 + i\omega \frac{\bar{\lambda}^2}{D}\right) \tag{13}$$

$$\bar{\lambda}^2 = \frac{\varepsilon k_B T}{\mathcal{N} q^2} \tag{14}$$

eq 11 generalizes eq 1 when the generation−recombination phenomenon is present and corresponds to a particular case of the more general expression reported in ref 9 (eq 32, that is equivalent to the analytic expression 40 of ref 9 in the completely blocking case) . The latter phenomenon is taken into account in the complex number Υ defined by eq 12. Note that, in the full dissociated case, where $k_a = 0$, $\kappa \to \infty$ and $\rho = 1$. In this case $\Upsilon = 1$ and $\xi = \beta$ are defined in eq 2. From eq 12, the real, Υ_R, and imaginary, Υ_I, parts of Υ are

$$\Upsilon_R = \frac{(k_d + 2k_a \mathcal{N})(k_d + k_a \mathcal{N}) + \omega^2}{(k_d + k_a \mathcal{N})^2 + \omega^2} \tag{15}$$

$$\Upsilon_I = -\frac{k_a \mathcal{N}}{(k_d + k_a \mathcal{N})^2 + \omega^2}\,\omega \tag{16}$$

respectively. From eqs 15 and 16, it follows that $\Upsilon_R > 0$ and $\Upsilon_I \leq 0$ for all ω. Furthermore, for $\omega \to 0$,

$$\Upsilon_R \to \frac{k_d + 2k_a \mathcal{N}}{k_d + k_a \mathcal{N}}, \text{ and } \Upsilon_I = 0 \tag{17}$$

whereas for $\omega \to \infty$,

$$\Upsilon_R \to 1, \text{ and } \Upsilon_I = 0. \tag{18}$$

Consequently, in the high-frequency regime, the generation−recombination effect does not play any role on the electrical impedance of the cell. The real part Υ_R is a monotonic decreasing function of ω, whereas Υ_I presents a minimum for $\omega = \omega^*$ defined by

$$\omega^* = k_d + k_a \mathcal{N} \tag{19}$$

For $\omega = \omega^*$, the real and imaginary components of Υ are

$$\Upsilon_R(\omega^*) = \frac{2k_d + 3k_a \mathcal{N}}{2(k_d + k_a \mathcal{N})} \tag{20}$$

$$\Upsilon_I(\omega^*) = -\frac{k_a \mathcal{N}}{2(k_d + k_a \mathcal{N})} \tag{21}$$

By means of the definition of $\kappa = k_d/(k_a \mathcal{N})$ and eq 10, it is possible to rewrite eqs20 and 21 in terms of the dissociation ratio ρ as follows

$$\Upsilon_R(\omega^*) = \frac{3 - \rho}{2} \tag{22}$$

$$\Upsilon_I(\omega^*) = -\frac{1 - \rho}{2} \tag{23}$$

In part a of Figure 2, we show the frequency dependencies of Υ_R and Υ_I. The dashed vertical line indicates the position of the

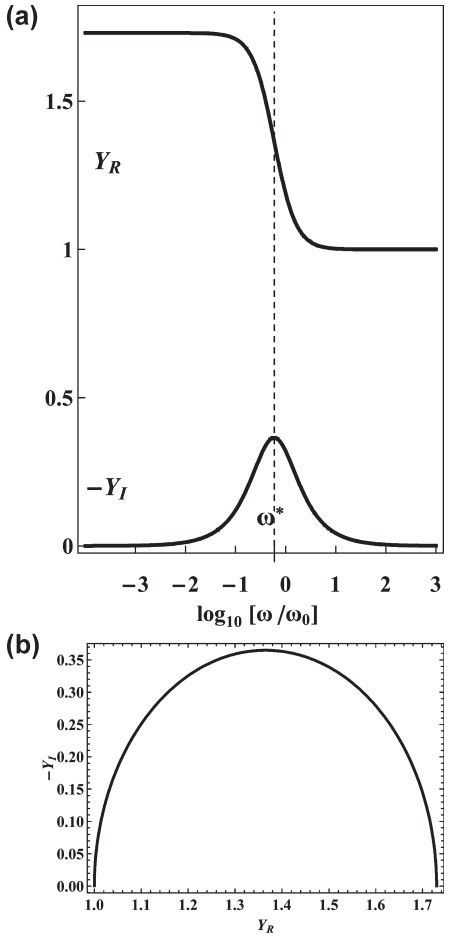

Figure 2. Frequency dependencies of Υ_R and Υ_I (a), and parametric plot of Υ_R versus Υ_I (b). $-\Upsilon_I$ has a local maximum at ω^* whose position is given by the vertical dashed line. ω_0 is a normalization circular frequency taken equal at 2π rad s^{-1}. $k = -21$, $k_d = 1$ s^{-1} and $\mathcal{N}_0 = 10^{22}$ m^{-3}.

circular frequency ω^* and it crosses the $-\Upsilon_I$ curve at its maximum. In part b of Figure 2 is reported the parametric plot of Υ_R versus Υ_I. For the numerical calculations we set $k_a = 10^{-21}$ m^3 s^{-1}, $k_d = 1$ s^{-1} and $\mathcal{N}_0 = 10^{22}$ m^{-3}.

Complex Wave Vector. Let us consider now the complex wave vector, whose square is defined in eq 13. Using eq 12, we get for the real, ξ_R^2, and imaginary, ξ_I^2, parts of ξ^2 the expressions

$$\xi_R^2 = \frac{(k_d + 2k_a\mathcal{N})(k_d + k_a\mathcal{N}) + \omega^2}{\bar{\lambda}^2[(k_d + k_a\mathcal{N})^2 + \omega^2]} + \frac{k_a\mathcal{N}}{(k_d + k_a\mathcal{N})^2 + \omega^2}\frac{\omega^2}{D} \quad (24)$$

$$\xi_I^2 = -\frac{k_a\mathcal{N}}{\bar{\lambda}^2[(k_d + k_a\mathcal{N})^2 + \omega^2]}\omega + \frac{(k_d + 2k_a\mathcal{N})(k_d + k_a\mathcal{N}) + \omega^2}{(k_d + k_a\mathcal{N})^2 + \omega^2}\frac{\omega}{D} \quad (25)$$

From eqs 24 and 25, we get that in the limit of $\omega \to 0$

$$\xi_R^2(0) = \frac{k_d + 2k_a\mathcal{N}}{\bar{\lambda}^2(k_d + k_a\mathcal{N})}, \text{and } \xi_I^2(0) = 0. \quad (26)$$

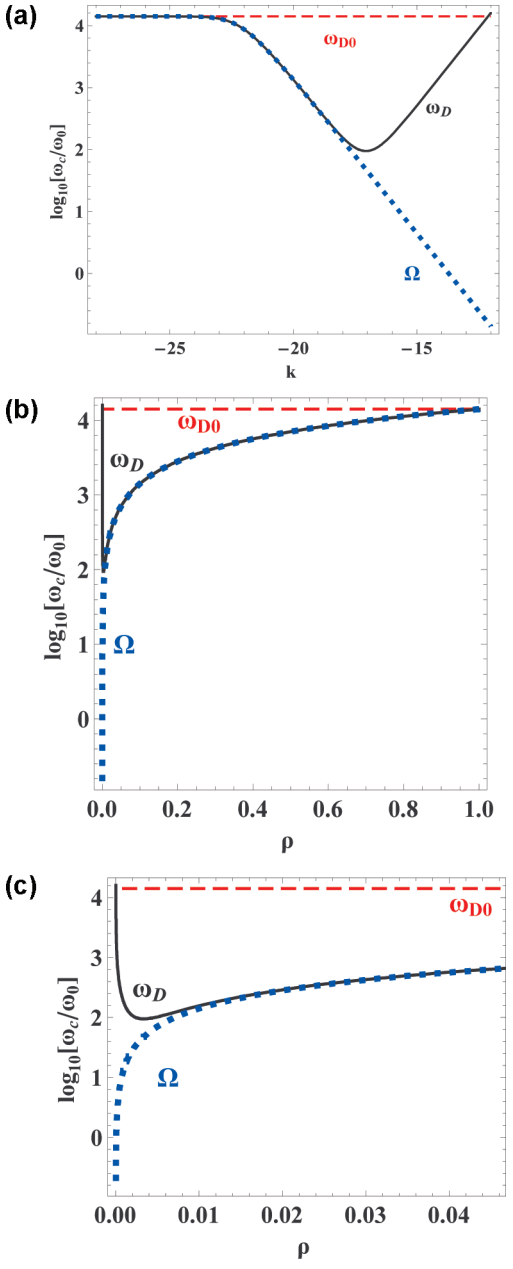

Figure 3. Comparison of the circular frequency of Debye for the full dissociated case, ω_{D0} (dashed red line), with the circular frequency of Debye (solid line) defined by eq 28 versus k, for $k_d = 1$ s^{-1} and $\mathcal{N}_0 = 10^{22}$ m^{-3}. The dotted blue line represents the circular frequency $\Omega = D/\bar{\lambda}^2$ (a). The same comparison is presented versus the dissociation ratio ρ in (b). Zoom of (b) in the range of small ρ, (c). In ω_c, c stands for D0, D, Ω. $\omega_0 = 2\pi$ rad s^{-1}.

In the opposite limit ω to ∞

$$\xi_R^2 = \frac{1}{\bar{\lambda}^2} + \frac{k_a\mathcal{N}}{D} + O(\omega^{-2}), \text{and } \xi_I^2 = \frac{\omega}{D} + O(\omega^{-1}) \quad (27)$$

As discussed in section II, in the case of fully dissociated impurities, at the circular frequency of Debye $\omega_{D0} = D/\bar{\lambda}_0^2$, the real and imaginary components of the complex wave vector β defined by eq 2 are equal. In the present case from eq 27, it follows that, in the high-frequency region, from the condition

dx.doi.org/10.1021/jp1094257 |J. Phys. Chem. B 2011, 115, 3496–3504

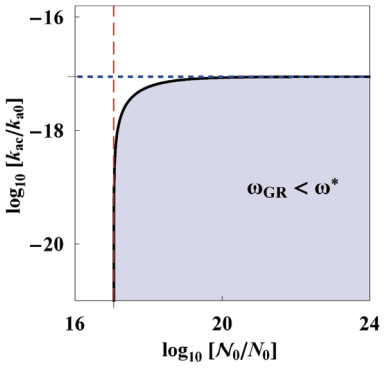

Figure 4. Dependence of the critical association coefficient k_{ac} on $\mathcal{N}_0$ (solid line). The horizontal asymptote corresponds to k_{ch}, and the vertical asymptote to k_d/k_{ch}. $k_d = 1\ s^{-1}$, $k_{a0} = 1\ m^3 s^{-1}$, and $\mathcal{N}_0 = 1\ m^{-3}$.

$\xi_R^2 = \xi_I^2$ we get that the actual circular frequency of Debye is

$$\omega_D = \frac{D}{\bar{\lambda}^2} + k_a \mathcal{N} \tag{28}$$

In part a of Figure 3, we compare the circular frequency of Debye for the full dissociate case, ω_{D0}, with the circular frequency of Debye defined by eq 28 versus the dimensionless quantity $k = \log_{10}(k_a/k_{a0})$, where the normalization quantity k_{a0} is taken equal to 1 $m^3 s^{-1}$. The numerical values of k_d, and $\mathcal{N}_0$ are the same as previously. In the same figure is also shown the circular frequency defined as $\Omega = D/\bar{\lambda}^2$ that gives a good approximation of ω_D for weak enough values of k. As expected, for small k, and hence dissociation ratio ρ close to 1, the three frequencies coincide. The same comparison is presented versus the dissociation ratio ρ in part b of Figure 3, whereas part c of Figure 3 is a zoom of part b of Figure 3 in the range of small ρ.

Critical Association Coefficient. A final remark on the complex wave vector ξ^2 is in order. From eqs26 and 27, it follows that ξ_R^2 is a monotonic decreasing function of ω if $\xi_R^2(0) > \xi_R^2(\infty)$, that implies

$$k_d + k_a \mathcal{N} < D/\bar{\lambda}^2 \tag{29}$$

Note that the first member of the inequality 29 coincides with ω^* defined in eq 19. This means that $\xi_R^2(\omega)$ is a decreasing function of ω only if the frequency related to the generation−recombination effect of ions $\omega_{GR} = \omega^* + k_a \mathcal{N} = k_d + 2k_a \mathcal{N}$ is smaller than ω_D defined by eq 28. By taking into account that $\mathcal{N} = \rho \mathcal{N}_0$ and the definition of ρ, from the inequality 29, we get that the association coefficient to observe the second plateau has to be smaller than a critical value k_{ac} given by

$$k_{ac} = \frac{D}{\mathcal{N}_0 \bar{\lambda}_0^2}\left(1 - \sqrt{\frac{k_d}{D}\bar{\lambda}_0}\right) \tag{30}$$

Let us now introduce a characteristic association coefficient defined by: $k_{ch} = Dq/(\varepsilon k_B T)$. Introducing the mobility μ of the ions by use of the Einstein−Smoluchowski relation,[20] the characteristic association coefficient can be equivalently written as $k_{ch} = \mu/\varepsilon$, that is, it depends only on the ionic mobility of the impurities and the dielectric constant of the host medium. Introducing k_{ch} the latter eq 30 can be cast in the form

$$k_{ac} = k_{ch}\left(1 - \sqrt{\frac{k_d}{k_{ch}\mathcal{N}_0}}\right) = k_{ch}(1 - \sqrt{\kappa_{ch}}) \tag{31}$$

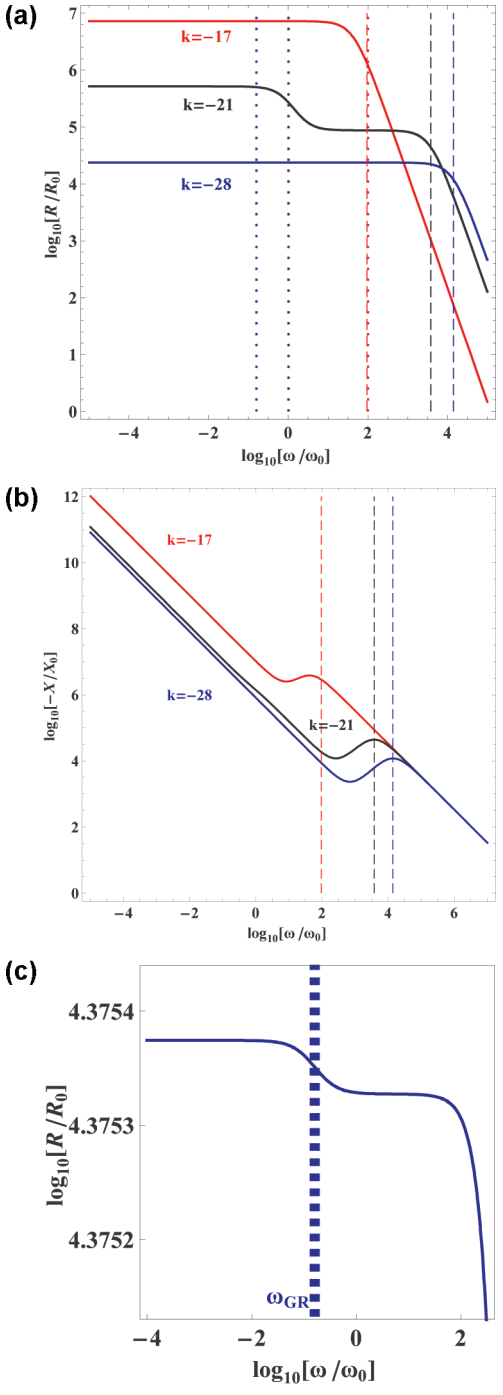

Figure 5. Frequency dependence of $R = \mathrm{Re}[Z]$ (a), and $X = \mathrm{Im}[Z]$ (b), for three values of $k = -17, -21, -28$. Dashed vertical lines indicate the position of ω_D. Dotted vertical lines indicate the position of ω_{GR}. (c), zoom of $R = \mathrm{Re}[Z]$ around ω_{GR} for $k = -28$. A plateau due to the generation recombination effect appears. $R_0 = 1$ ohm, $X_0 = 1$ ohm, and $\omega_0 = 2\pi$ rad s^{-1}.

Note that k_{ch} fixes un upper limit for k_{ac} above which the second plateau disappears. Further, k_{ac} becomes 0 when $\kappa_{ch} = 1$, that is, given the ionic mobility, the dielectric constant of the medium and the dissociation coefficient, a value for the bulk density of dissociable particles $\mathcal{N}_{0L}$ is fixed below which no plateau exists.

Figure 4 shows the dependence of k_{ac} on $\mathcal{N}_0$ (solid line). In the filled part of the diagram, where $\omega_{GR} < \omega^*$, a second plateau

dx.doi.org/10.1021/jp1094257 |J. Phys. Chem. B 2011, 115, 3496–3504

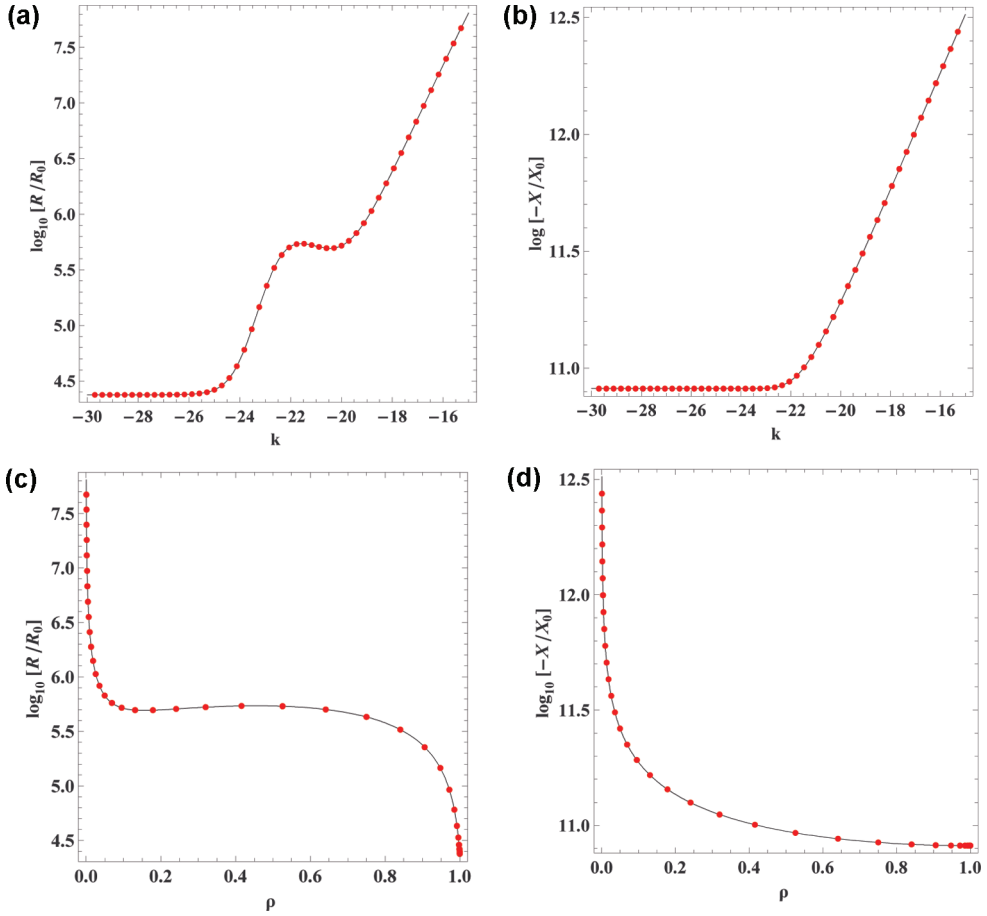

Figure 6. Comparison of the predictions of the exact (solid point curve) and approximate (solid line curve) formula for R, (a), and X, (b), versus k, at $\omega = 2\pi^{*}10^{-5}$ rad/s. In (c) and (d) the comparison is done versus the dissociation ratio ρ. The two curves coincide in the full range of k, or of ρ, indicating that in the considered limit the approximated expressions work well.

exists. The horizontal asymptote for $\mathcal{N}_0 \rightarrow \infty$ gives the value of k_{ch}. The vertical asymptote is the line $\mathcal{N}_{0L} = k_d/k_{ch}$ that gives the lowest value of $\mathcal{N}_0$ for which a second plateau could be observed. The numerical value of k_{ch} is 8.85×10^{-18} $m^3 s^{-1}$ and of the lowest bulk density of dissociable particles $\mathcal{N}_{0L}$ is 1.13×10^{17} m^{-3}.

IV. SPECTRA OF THE REAL AND IMAGINARY PARTS OF Z

To investigate the impedance of the cell that is given by eq 11, in the presence of the generation−recombination phenomenon we use the following values for the parameters of the model: $k_d = 1\ s^{-1}$, $\mathcal{N}_0 = 10^{22}\ m^{-3}$, $\varepsilon = 6.7\varepsilon_0$, and $D = 8.2 \times 10^{-11}\ m^2\ s^{-1}$, $d = 25 \times 10^{-6}$ m, and $S = 2 \times 10^{-4}\ m^2$, as in ref [10]. Figure 5 shows the spectra for $R = \mathrm{Re}[Z]$ (a), and $X = \mathrm{Im}[Z]$ (b), for three values of $k = \log_{10}(k_a/k_{a0})$: $k = -28$, -21, and -18. The results shown in part a of Figure 5 are similar to some of those reported.[9,10] This figure seems to imply that for large and small values of k, $R = R(\omega)$ presents just a plateau, whereas for intermediate values of k, $R = R(\omega)$ presents two plateau. A simple numerical investigation shows that when the two plateaus are present, one ends at the circular frequency ω_{GR}, and the other at circular frequency ω_D, discussed above. The position of these frequencies is noted in the figure by vertical dashed lines for ω_D, and by vertical dotted lines for ω_{GR}. Actually, for $k = -28$ the second plateau exists as it is shown in a zoom of Figure part a of 5 around ω_{GR}, as seen in part c of Figure 5. Note that, for the case $k = -17$, a second plateau cannot exist because $\omega_{GR} > \omega^{*}$ (or $k_a/k_{ch} = 1.13 > 1$). Finally, note that ω_D, represented by a vertical dashed line for each value of k, in part b of Figure 5 gives the position of the local maximum of the curve $-X(\omega)$ when $\omega_{GR} < \omega_D$ but this is no longer the case when the latter inequality is violated, case $k = -17$.

Frequency-Limiting Behavior. In the limit of $\omega \rightarrow 0$ from the expression 11, we get for R and X the expressions

$$R_L = \frac{\overline{\lambda}}{\varepsilon D S}(d\overline{\lambda} + \Delta,) \tag{32}$$

where

$$\Delta = \sqrt{\frac{k_d + k_a\mathcal{N}}{k_d + 2k_a\mathcal{N}}}\left\{\frac{Dk_a\mathcal{N}}{(k_d + k_a\mathcal{N})(k_d + 2k_a\mathcal{N})} - 3\overline{\lambda}^2\right\} \tag{33}$$

and

$$X_L = -\frac{1}{\omega}2\frac{\overline{\lambda}}{\varepsilon S}\sqrt{\frac{k_d + k_a\mathcal{N}}{k_d + 2k_a\mathcal{N}}} \tag{34}$$

valid in the limit where

$$n_c = \frac{d}{2\overline{\lambda}}\sqrt{\frac{k_d + k_a\mathcal{N}}{k_d + 2k_a\mathcal{N}}} \gg 1. \tag{35}$$

dx.doi.org/10.1021/jp1094257 |J. Phys. Chem. B 2011, 115, 3496–3504

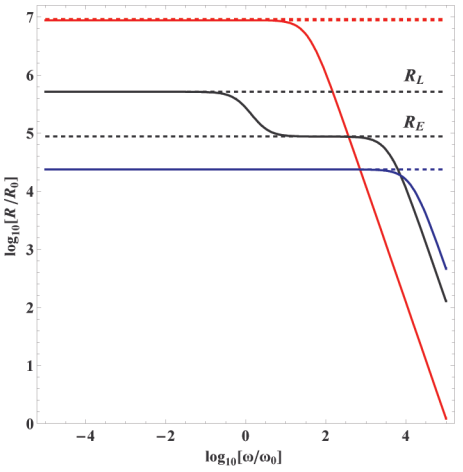

Figure 7. $R(\omega)$ calculated for the same three values of k as in Figure 4. The horizontal dashed lines represent, R_L, and R_E. When the second plateau exists, its value coincides with R_E. $R_0 = 1$ ohm, and $\omega_0 = 2\pi$ rad s^{-1}.

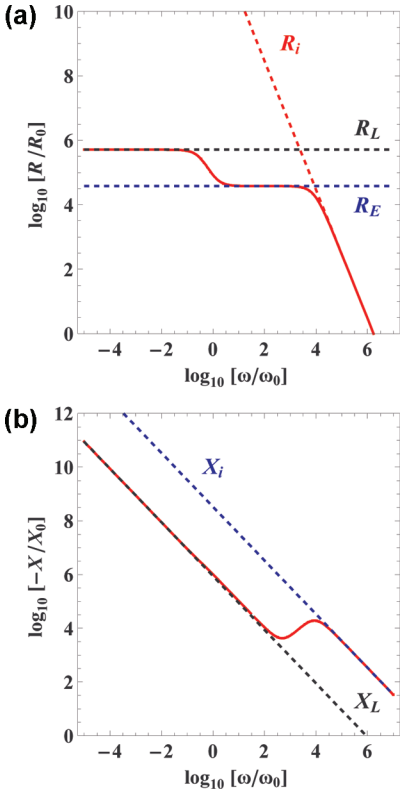

Figure 8. Spectra of R, (a), and X, (b), versus the normalized circular frequency calculated from the exact formula. The dashed lines are calculated from the approximated expressions that are valid in the low- and high-frequency range. In the spectrum of $R(\omega)$ is reported also the value of R_E, (a). The numerical value of k used in the numerical calculations is -22. $R_0 = 1$ ohm, $X_0 = 1$ ohm, and $\omega_0 = 2\pi$ rad s^{-1}.

In parts a and b of Figure 6, we compare, in the limit of small omega ($\omega = 2\pi \times 10^{-5}$ rad/s) the exact values of R and X deduced by means of eq 11 with the approximated formulas 32 and 34 for different values of k. The solid points are calculated from eq 11, whereas the solid lines from the approximated formulas. In parts c and d of Figure 6, the comparison is shown also versus the dissociation ratio ρ. As it is evident from Figure 6, the agreement between the two formulas is rather good for all values of k and for all values of ρ.

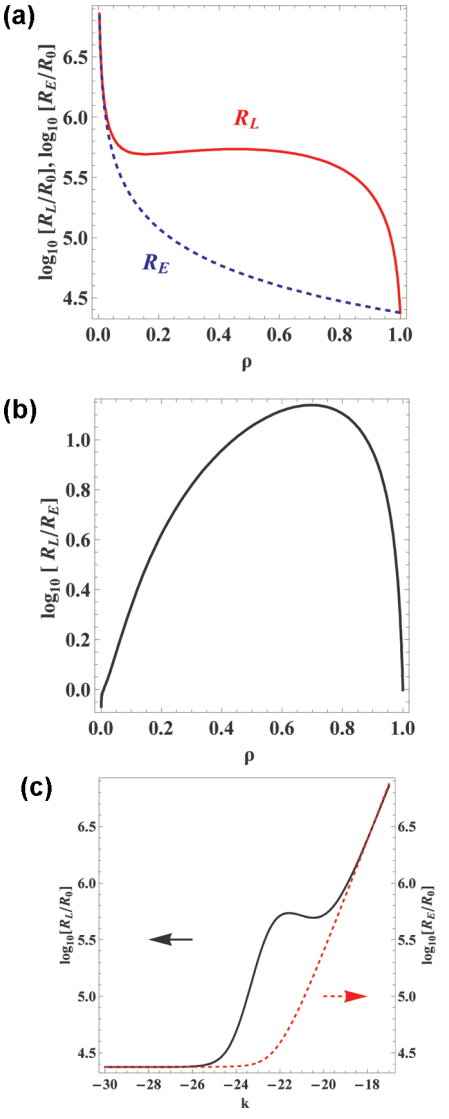

Figure 9. R_L (solid line) and R_E (dashed line) versus the dissociation ratio ρ, (a), the ratio R_L/R_E versus ρ, (b), and R_L (solid line) and R_E (dashed line) versus k (c). $R_0 = 1$ ohm.

If the term in Δ can be neglected, from eq 32 we obtain for R_E the expression

$$R_E = d\frac{\overline{\lambda}^2}{\varepsilon DS} \tag{36}$$

that reminds expression 3 in the $\omega \rightarrow 0$, for the full dissociated case. In Figure 7 are shown by solid lines R, and by dashed lines R_L, and R_E versus ω for the same three values of k as in Figure 5. When the second plateau exists, its value coincides with R_E. The critical number n_c, as defined in 35, is of the order of 29, 280, and 420, for $k = -17$, $k = -21$, and $k = -28$, respectively.

dx.doi.org/10.1021/jp1094257 |J. Phys. Chem. B 2011, 115, 3496–3504

In the limit of $\omega \rightarrow \infty$, from eq 11 we get for the leading terms of R and X the expressions

$$R_i \sim \left(\frac{D}{\bar{\lambda}^2} + k_a \mathcal{N}\right)\frac{d}{\varepsilon S}\frac{1}{\omega^2} \tag{37}$$

$$X_i \sim -\frac{1}{\omega}\frac{d}{\varepsilon S}. \tag{38}$$

In Figure 8, we compare the spectra of $R(\omega)$, (a), and $X(\omega)$, (b), calculated from eq 11 (solid lines) with the limiting expressions (dashed lines) given by eqs 32 and 34 and eqs 37 and 38. In part a of Figure 8 is also reported R_E calculated from eq 36. The figure has been drawn for $k = -22$.

As shown in part a of Figure 6, in the low-frequency range, the value of R evaluated by means of the exact formula for Z given by eq 11 coincides with the one obtained with the approximated formula 32. For some values of k, or of the dissociation ratio ρ, there is also another plateau, well described by R_E given by eq 36. Our aim is now to evaluate how the ratio

$$r = \frac{R_L}{R_E} = 1 + \frac{\Delta}{d\bar{\lambda}} \tag{39}$$

depends on ρ. This calculation can be performed analytically only when the critical number $n_c \gg 1$, because in this case expressions 32 and 34 hold. We will estimate in the following for what value of ρ, or of k this condition is fulfilled. We will perform now the analysis in term of the dissociation ratio ρ.

The quantity Δ and the critical number n_c, defined by means of eqs 33 and 35, can be rewritten in terms of the dissociation ratio ρ as

$$\Delta = \frac{1}{\rho\sqrt{2-\rho}}\left\{\frac{(1-\rho)\rho^2}{2-\rho} - 3\frac{k_d\bar{\lambda}_0^2}{D}\right\}\frac{D}{k_d} \tag{40}$$

$$n_c = \frac{d}{2\bar{\lambda}_0}\sqrt{\rho(2-\rho)} \tag{41}$$

respectively.

Because R_E is defined by eq 36, $r \geq 1$ implies $\Delta \geq 0$, and, hence, using eq 40,

$$\frac{(1-\rho)\rho^2}{2-\rho} - 3\frac{k_d\bar{\lambda}_0^2}{D} \geq 0. \tag{42}$$

that defines the maximum, ρ_M, and minimum, ρ_m, values of ρ for which $r \geq 1$. Using the same values of the model parameters as before, we obtain $\rho_M \sim 0.999966$, and $\rho_m \sim 0.00825$. The relevant values of k_a are, for ρ_M, $k_{am} \sim 3.39 \times 10^{-27}$ m^3 s^{-1}, and for ρ_m, $k_{aM} \sim 1.457 \times 10^{-18}$ m^3 s^{-1}. The critical number $n_r(\rho)$, is then $n_r(\rho_M) \sim 400$, and $n_r(\rho_m) \sim 29$. Because $n_r(\rho_m)$ is not large enough, eq 32 does not give a good approximation for the exact formula 11 when $\rho = \rho_{min}$.

Further, when the approximated formula for R works well, it is possible to evaluate the dissociation ratio for which r is maximum. Using eq 40, we get that the maximum of r is reached for $\rho = \rho^+$ belonging to the interval $\rho_m \leq \rho^+ \leq \rho_M$, whose order of magnitude is fixed by the maximum of 42. A simple calculation gives

$$\rho^+ \sim \frac{7-\sqrt{17}}{4} \sim 0.719. \tag{43}$$

In Figure 9, we show R_L and R_E versus ρ, (a), $r = R_L/R_E$ versus ρ, (b), and R_L and R_E versus k, (c). For very small values of ρ, the quantity $r = R_L/R_E$ decreases below 1, that is, $R_L < R_E$ (part b of Figure 9). This result seems to indicate that there is an inversion of the two plateaus. However, this result is related to the circumstance that in this limit the approximate formula 32 is no longer reliable because the condition 35 is not verified.

For the set of physical parameters used in the numerical calculations, the spectrum of $R = R(\omega)$ presents two plateaus for $\rho_m \leq \rho \leq \rho_M$, or for $k_{am} \leq k_a \leq k_{aM}$.

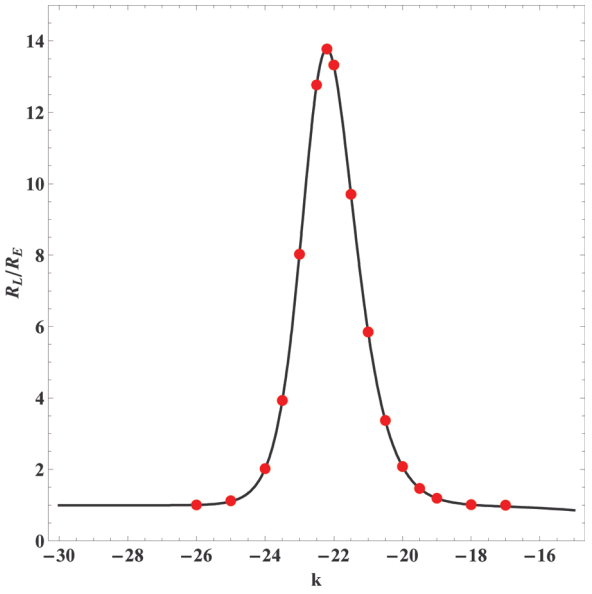

Figure 10. R_L/R_E dependence on k. Solid points are data generated by the *LEVM* program.[11] Solid line is calculated from the present model using the same parameters as in ref 11. No fitting has been performed.

Comparison of the Two Models. Figure 10 shows for comparison the R_L/R_E dependence on k calculated analytically by the present model and by the model.[11] The solid red points are data generated by the *LEVM* program[21] and kindly communicated to us by J.Ross Macdonald. For the calculations, J. Ross Macdonald uses the $R(\omega)$ data generated by the *LEVM* program[21] to evaluate the value of the R_L/R_E ratio as function of k. The black solid line is calculated analytically from eq 39 of the present model using the same parameters as in ref11. Because no fitting has been performed, one notes the excellent agreement of the two models. Further comparison (not presented here) of the results obtained from both models implies that the analytical expressions for the impedance including generation−recombination effects of[1,8,9] are equivalent to the eq 11 of the present model.

V. DISCUSSION AND CONCLUSIONS

We have discussed the importance of the generation−recombination phenomenon on the spectra of the real and imaginary parts of the electrical impedance of a cell of material containing dissociable impurities. The analysis has been performed, for

simplicity, by assuming that the cell is in the shape of a slab, with perfectly blocking electrodes. We have assumed, furthermore, that only one type of ions is mobile. In this aspect, our calculation is valid for a gel containing impurities that can dissociate in two ions and that this dissociation−association reaction is of first type. In this framework, we have shown that the generation−recombination phenomenon can be responsible for the appearance of a second plateau of the real part of the impedance, in the series representation. We have evaluated the values of the resistance corresponding to the two plateaus, and the frequencies at which the plateaus end. Our results are in agreement with those reported by Ross Macdonald et al.,[8] and recently published by Ross Macdonald,[11] where the more general situation of two mobile ions is considered. We also calculated the existence range of the GR-plateau. A preliminary discussion on the observability of the GR-effect in connection with materials and charge carriers types was reported in ref 8. As discussed in refs 22 and 23, when the diffusion coefficients of the positive and negative ions are different, even in the absence of the generation−recombination phenomenon, the real part of the impedance can present two plateaus: one related to the free diffusion, and the other due to the ambipolar diffusion. In ref 11, it is shown numerically that, in the case of two mobile ions, with different diffusion coefficients, the presence of the generation−recombination phenomenon gives rise to a third plateau. A similar effect is expected when more than two groups of ions are present in the medium under consideration, as discussed in ref 24. Therefore, even if the r ratio for $-23 \leq k \leq -21$ is large enough (Figure 10) the GR-plateau may be hidden from the presence of other effects such as ambipolar diffusion, electrode polarization, and so forth. To observe the GR-plateau one has to carefully design an experiment looking to eliminate some of the concurrent effects.

■ ACKNOWLEDGMENT

Many thanks are due to J. Ross Macdonald for fruitful discussions on the generation−recombination phenomenon and for useful indications on the existing bibliography on the subject. I.L. acknowledges the Special Account for Research Grants of the National and Kapodistrian University of Athens for financial support. This work has been partially supported by Regione Piemonte, Direzione Sanitá, Settore Promozione della Salute e Interventi di Prevenzione Individuale e Collettiva, in the frame of the project "*Study of the electrical properties of the interface electrode-skin*".

■ REFERENCES

(1) Macdonald, J. Ross *Phys. Rev.* **1953**, *92*, 4.
(2) All the works of Macdonald are accessible, in pdf format, at http://jrossmacdonald.com
(3) Macdonald, J. Ross *J. Electroanal. Chem.* **1976**, *70*, 17.
(4) Macdonald, J. Ross; Jacobs, P. W. M. *J. Phys. Chem. Solids* **1976**, *37*, 1117.
(5) Franceschetti, D. R.; Buck, R. P.; Macdonald, J. Ross *J. Electrochem. Soc.* **1991**, *138*, 1368.
(6) Macdonald, J. Ross *J. Electrochem. Soc.* **1988**, *135*, 2274.
(7) Franceschetti, D. R.; Macdonald, J. Ross *J. Appl. Phys.* **1979**, *50*, 291.
(8) Macdonald, J. Ross; Franceschetti, D. R.; Meaudre, R. *J. Phys. C: Solid State Phys.* **1977**, *10*, 1459.
(9) Macdonald, J. Ross; Franceschetti, D. R. *J. Chem. Phys.* **1978**, *68*, 1614.
(10) Derfel, G.; Kaminski Lenzi, E.; Refosco Yednak, C.; Barbero, G. *J. Chem. Phys.* **2010**, *132*, 224901.
(11) Macdonald, J. Ross *J. Phys.: Condens. Matter* **2010**, *22*, 495101.
(12) Barbero, G. *Phys. Rev. E* **2005**, *71*, 062201.
(13) Chang, H.; Jaffé, G. *J. Chem. Phys.* **1952**, *20*, 1071.
(14) Barbero, G.; Batalioto, F.; Figueiredo Neto, A. M. *J. Appl. Phys.* **2007**, *101*, 054102.
(15) Barbero, G.; Alexe-Ionescu, A. L.; Lelidis, I. *J. Appl. Phys.* **2005**, *98*, 113703.
(16) Cirkel, P. A.; van der Ploeg, J. P. M.; Koper, G. J. M. *Physica A* **1997**, *235*, 269.
(17) Barbero, G.; Alexe-Ionescu, A. L. *Liq. Cryst.* **2005**, *32*, 943.
(18) Macdonald, J. Ross *J. Electroanal. Chem.* **1971**, *32*, 317.
(19) Macdonald, J. Ross *J. Appl. Phys.* **2010**, *107*, 101101.
(20) Atkins, P. W. *Physical Chemistry*; Oxford University Press: Oxford, 2000.
(21) J. Ross Macdonald, CNLS (Complex Nonlinear Last Squares) Immittance, Inversion and Simulation Fitting Program for MS WINDOW, MS-DOS, v.8.10, available at: http://jrossmacdonald.com/levm.html.
(22) Lelidis, I.; Barbero, G. *Phys. Lett. A* **2005**, *343*, 440.
(23) Barbero, G.; Lelidis, I. *Phys. Rev. E* **2007**, *76*, 051501.
(24) Barbero, G.; Batalioto, F.; Figueiredo Neto, A. M. *Appl. Phys. Lett.* **2008**, *92*, 172908.